Synthesis and structures of samarium platinum germanides: $SmPtGe_2$ and $Sm_2Pt_3Ge_5$

Fumiko Ohtsu, Hiroshi Fukuoka*, and Shoji Yamanaka

Department of Applied Chemistry, Graduate School of Engineering, Hiroshima University, Higashi-Hiroshima 739-8527, Japan

Abstract

We performed single-crystal structure analysis of two ternary samarium platinum germanides $SmPtGe_2$ and $Sm_2Pt_3Ge_5$. $SmPtGe_2$ crystallizes in the space group (S.G.) *Immm* (No. 71) with a = 4.3679(9) Å, b = 8.728(2) Å, c = 16.378(4) Å, and V = 624.4(2) Å^3. This compound is isotypic with $YIrGe_2$ having a $Ge_{10}Pt_4$ subunit composed of edge-sharing five- and six-membered rings. $SmPtGe_2$ shows a metallic conductivity from room temperature down to 2 K. The magnetic susceptibility measurement showed a 3+ oxidation state for the samarium. $Sm_2Pt_3Ge_5$ crystallizes in the S.G. *Ibam* (No. 72) with a = 10.174(1) Å, b = 11.761(2) Å, c = 6.2142(8) Å, and V = 743.6(2) Å^3. It is isotypic with $U_2Co_3Si_5$ with a structure closely related to $ThCr_2Si_2$.

Keywords: Germanide; samarium platinum germanide; single crystal; structure analysis

1. Introduction

Binary germanides of electropositive elements, such as alkali, alkaline earth, and rare earth metals, show various networks composed of Ge–Ge covalent bonds. Such networks are usually composed of three- and four-bonded Ge atoms. The network in $LaGe_2$ with the α–$ThSi_2$ structure contains only three-bonded trigonal Ge atoms [1]. Ba_8Ge_{43} with the type I clathrate structure and $SrGe_{6-\delta}$ contain three- and four-bonded tetragonal Ge atoms [2-4]. Recently, eight-bonded Ge atoms were found in $LnGe_5$ (*Ln* = La, Ce, Pr, Nd, and Sm) [5, 6]. The structural diversity of binary germanides is mainly due to this structural flexibility of germanium atoms.

In ternary germanide systems, the addition of coin metals and platinum is interesting in terms of the structural diversity. These metals can participate in the Ge networks in two ways. First, they take specific coordination forms that can be distinguished clearly from those of Ge. Platinum–germanium skutterudite compounds such as $BaPt_4Ge_{12}$ are examples of such cases [7, 8]. In $BaPt_4Ge_{12}$, each platinum atom is octahedrally coordinated by six Ge atoms. On the other hand, Ge atoms can form Ge_4 units with a rectangular shape. The difference in the structural environments of Pt and Ge is obvious in this compound. Recently, $BaPt_4Ge_{12}$ and its related compounds, APt_4Ge_{12} (A = Sr, La, Pr, and Th), have attracted much attention owing to their superconductivity [7-10].

The second example, coin and platinum metals can substitute Ge sites to form combined frameworks, as seen in $Ba_8M_6Ge_{40}$ (M = Pt, Au, Ag, and Cu) [11]. In these compounds, each M atom is tetrahedrally coordinated by four Ge atoms having similar tetrahedral coordinations. This structure can be understood as a derivative of the imaginary Ba_8Ge_{46}; Pt atoms substitute six Ge atoms per one unit cell and participate in the Ge covalent network [11]. APt_2Ge_2 type compounds with the $ThCr_2Si_2$ and $LaPt_2Ge_2$ structures are other examples [12, 13]. Pt and Ge atoms occupy different sites, but their chemical environments are similar. They combine to form host networks.

Based on this perspective, structural studies of ternary germanides of platinum metals are an interesting theme in germanide chemistry. In this study, we have investigated the reactions of the Sm–Pt–Ge ternary system using high-pressure techniques and a simple arc-melting method. Reflecting the structural flexibility mentioned above, many ternary compounds have been reported in this system. SmPtGe crystallizes in two forms: the YPdSi and TiNiSi structures [14]. $SmPt_xGe_{2-x}$

forms the α–$ThSi_2$ and AlB_2 structures, and when x < 0.25, it forms the α–$ThSi_2$ structure [15]. $SmPt_2Ge_2$ has two crystal forms, $LaPt_2Ge_2$ (monoclinic) and $CaBe_2Ge_2$ (orthorhombic) types, which are derivatives of the $ThCr_2Si_2$ structure [16]. $SmPtGe_2$ and $Sm_2Pt_3Ge_5$ have been reported to crystallize in the $YIrGe_2$ and $U_2Co_3Ge_5$ structures, respectively, although the structural analysis has yet to be performed for these compounds [17, 18]. In this study, we successfully obtained single crystals of $SmPtGe_2$ and $Sm_2Pt_3Ge_5$ and performed single crystal structural analysis.

2. Experimental

Mixtures of Sm, Pt, and Ge with various atomic ratios were melted in an Ar-filled arc furnace. The purity of all chemicals used was greater than 99.9%. Products were characterized by powder XRD measurements performed on a Burker D8 Advance diffractometer with Cu Kα radiation.

High-pressure and -temperature reactions were performed using Kawai-type 6-8 cells at 10 to 13 GPa. We placed starting mixtures of $SmGe_2$ and Ge with appropriate ratios into h-BN containers. The container was then placed in an octahedral-shaped MgO cell and reacted in a Kawai-type high-pressure system. The details of such high-pressure techniques are described elsewhere [19].

Single-crystal X-ray analysis was performed using a Rigaku R-AXIS diffractometer equipped with an imaging plate area detector with graphite-monochromated MoKα radiation. Single-crystal structure analysis was performed using the SHELX-97 crystallographic software package [20], and an empirical absorption correction was applied. The structure was solved by direct methods and expanded using Fourier techniques.

Chemical compositions of the products were determined using an electron probe microanalyzer (EPMA) (JEOL JCMA-733). Electrical resistivity was measured on a specimen with dimensions of 0.5 × 0.8 × 1.1 mm^3 by a typical four-probe method using DC from 2 to 300 K. Magnetic susceptibility measurements were performed using a SQUID magnetometer (Quantum Design MPMS-5) in a 5000-Oe field.

3. Results and discussion

3.1. Structure, electrical and magnetic properties of $SmPtGe_2$

$SmPtGe_2$ was obtained by arc-melting of an Sm:Pt:Ge = 1:1:2 mixture. It was however difficult to obtain single crystals suitable for the structure analysis. Although high-pressure conditions are not necessary for the synthesis of this compound, good single crystals of $SmPtGe_2$ could be obtained by reaction at 13 GPa and 1200°C from an Sm:Pt:Ge = 1:1:3 mixture. The excess amount of Ge probably acted as a good flux for the crystal growth of $SmPtGe_2$. A dark gray single crystal with dimensions of 0.02 × 0.02 × 0.04 mm^3 was used for structure analysis. Crystallographic data, atomic parameters, and atomic displacement parameters are listed in Tables 1, 2, and 3.

$SmPtGe_2$ crystallizes in the space group (S.G.) *Immm* with lattice constants a = 4.3679(9) Å, b = 8.728(2) Å, c = 16.378(4) Å, and V = 624.4(2) $Å^3$. The composition of the compound analyzed by EPMA was Sm:Pt:Ge = 1:1:2. The crystal structure of $SmPtGe_2$ is shown in Fig. 1. The structure contains three crystallographically independent Ge sites. One is four-bonded Ge (Ge1 site) and two are three-bonded Ge (Ge2 and Ge3 sites). Ge–Ge distances are in the range from 2.439(5) to 2.620(3) Å. All Pt atoms are in equivalent sites and each Pt atom is coordinated by five Ge atoms with distances of 2.4808(9), 2.486(2), and 2.510(1) Å. No Pt–Pt bond exists in the network.

There are two samarium sites (Sm1 and Sm2). The local structures around them are shown in Fig. 2. The Sm1 atom is sandwiched between two five-membered rings and is surrounded by 14 Ge and Pt atoms with distances of 3.019(1) to 3.254(1) Å. On the other hand, the Sm2 atom is sandwiched between two six-membered rings and surrounded by 12 Ge and Pt atoms with distances of 3.270(1) to 3.2738(7) Å.

The structure can be easily understood using the subunit $Ge_{10}Pt_4$ (see Fig. 1), as pointed out by François et al. about isotypic $YIrGe_2$ [17]. This planar subunit contains two six-membered and two five-membered rings sharing their Ge2–Ge2 and Ge3–Ge3 edges. These units are mutually connected by sharing those edges to form $[Ge_8Pt_4]_\infty$ blocks. The blocks are connected to one another by bonds between Ge2 and Pt atoms to form the entire structure with large spaces where Sm ions are situated.

We observed large thermal displacement parameters U_{11} for the Ge2 and Ge3 atoms (Table 3). Especially, the U_{11} of Ge2 (0.054(2)) is fairly large, and the thermal ellipsoid of Ge2 is elongated along the a-axis (Fig. 2(b)). These Ge atoms are on the shared-edges of $[Ge_8Pt_4]_\infty$ blocks, indicating

that the flat formation of the $[Ge_8Pt_4]_\infty$ block is unstable and the six-membered rings in the unit tend to be puckered.

The electrical resistivity of $SmPtGe_2$ in the range from 2 to 300 K is shown in Fig. 3. The measurement was performed using an $SmPtGe_2$ sample obtained by arc-melting an Sm:Pt:Ge = 1:1:2 mixture. The resistivity decreases with temperature, indicating that it is metallic. Magnetic susceptibility measurement was also performed using the same arc-melted sample. The temperature dependence of the magnetic susceptibility of $SmPtGe_2$ does not obey the Curie–Weiss law (Fig. 4), possibly because of the first- and second-order Zeeman effects of Sm^{3+}. A small anomaly observed at 11 K is most likely due to an impurity. When discussing the temperature dependence of the magnetic susceptibility of Sm^{3+} (^6H term of f^4), the first- and second-order Zeeman effect for the J = 5/2 and 7/2 states should be considered. Below room temperature, the high-order terms of the theoretical equation can be ignored, and we can approximate it by the following equation:

$$(1)\quad \chi_{mol}(T) \approx \frac{N_A\mu_B{}^2 / 3k \{4.286 / T + 14.694\, k / \lambda + (85.841 / T + 3.281\, k / \lambda) \exp(-7\lambda / 2kT)\}}{6 + 8 \exp(-7\lambda / 2kT)}$$

where N_A is Avogadro's number, μ_B is the Bohr magneton, k is the Boltzmann constant, and λ is the spin-orbit coupling constant [21]. The second term corresponds to the well-known temperature independent paramagnetism or Van Vleck paramagnetism. The theoretical magnetic susceptibility derived from Equation (1) with $\lambda = 236\ cm^{-1}$ is shown in Fig. 4. Although the experimental data did not show a perfect correspondence to theoretical data, the tendency is very similar. The observed effective magnetic moment at room temperature is 1.58 μ_B, which is well corresponding to the theoretical value for Sm^{3+} (1.55 μ_B).

3.2. Structure of $Sm_2Pt_3Ge_5$

Single crystals of $Sm_2Pt_3Ge_5$ were obtained from a mixture of Sm:Pt:Ge = 1:1:3. The mixture was allowed to react under a pressure of 13 GPa. The temperature was maintained at 1000°C for 1 hour and then decreased from 1000 to 850°C over 1 hour, followed by quenching at room temperature. After cooling, the pressure was slowly released. The composition analyzed by EPMA is Sm:Pt:Ge = 2:3:5. A dark gray single crystal with dimensions $0.01 \times 0.01 \times 0.02\ mm^3$ was used

for the structure analysis. Crystallographic data, atomic parameters, and atomic displacement parameters are listed in Tables 1, 4, and 5.

$Sm_2Pt_3Ge_5$ is isotypic with the $U_2Co_3Si_5$ structure. Kurenbaeva et al. reported synthesis and lattice constants of $SmPt_{1.75}Ge_{2.25}$ with the $U_2Co_3Si_5$ structure, though the structural details were not reported [18]. Our compound is isotypic with $SmPt_{1.75}Ge_{2.25}$, but the composition differs. This alteration is probably due to the difference in the preparation conditions. (Their sample was prepared by arc-melting followed by annealing at 597ºC in quartz ampoule.)

The crystal structure of $Sm_2Pt_3Ge_5$ is shown in Fig. 5. It is closely related to the $ThCr_2Si_2$ and $BaAl_4$ structures. The network is composed of crystallographically independent two-Pt and three-Ge sites. Each Pt1 and Pt2 atom is coordinated by six and five Ge atoms, respectively. The Ge1 atom is coordinated by four Pt2 atoms. On the other hand, the Ge2 and Ge3 atoms have five-fold coordination with three Pt and two Ge atoms. There is no Pt – Pt bond as in $SmPtGe_2$. Each Sm atom has 14 neighboring atoms (10 Ge and 4 Pt) with distances of 3.016(2) to 3.391(2) Å.

The chemical surroundings around Pt2 and Ge3 are very similar. The bond between these atoms has the shortest Pt–Ge distance (2.412(2) Å). The other Pt-Ge distances are observed in the range from 2.485(1) to 2.536(1) Å. There is only one Ge–Ge distance (Ge2–Ge3 2.640(2) Å), which is much longer than the Ge – Pt distances in spite of the similarity of their covalent radii (1.30 (Pt) and 1.22 (Ge) Å). This difference is probably due to the electronegativity of these elements. In germanides, host networks have the net negative charge donated from guest cations. The charge is distributed on host atoms according to their electronegativity. Because germanium is more electronegative than platinum in germanides, the effective radii of Ge becomes larger than that of Pt. This phenomenon is often observed for ternary platinum germanides.

4. Conclusions

Single crystals of $SmPtGe_2$ and $Sm_2Pt_3Ge_5$ were prepared with the aid of high-pressure reaction techniques. $SmPtGe_2$ crystallizes in the $YIrGe_2$ structure and contains a subunit $Ge_{10}Pt_4$ composed of edge-sharing five- and six-membered rings. We confirmed the oxidation state of Sm^{3+} by the magnetic susceptibility measurement. $SmPtGe_2$ shows metallic properties. $Sm_2Pt_3Ge_5$ has the

$U_2Co_3Si_5$ structure.

Acknowledgments

We are grateful to Mr. Yasuhiro Shibata of Hiroshima University for his help with the EPMA measurements. This work was supported by a Grant-in-Aid for Scientific Research from the Ministry of Education, Culture, Sports, Science, and Technology of Japan, Grant No. 16037212, 16750174, 18750182, 18027010, and 20550178.

References

[1] E.I.Gladyshevskii, J. Struct. Chem. 5 (1964) 523-529.

[2] W. Carrillo-Cabrera, S.Budnyk, Y.Prots, and Y. Grin, Z. Anorg. Allg. Chem. 630 (2004) 2267-2276.

[3] H. Fukuoka, J. Kiyoto, and S. Yamanaka, J. Phys. Chem. Solid 65 (2004) 333-336.

[4] H. Fukuoka, S. Yamanaka, E. Matsuoka, and T. Takabatake, Inorg. Chem. 44 (2005) 1460-1465.

[5] H. Fukuoka, S. Yamanaka, Phys Rev. B67 (2003) 0945011-0945015.

[6] H. Fukuoka, K. Baba, M. Yoshikawa, F. Ohtsu, and S. Yamanaka, J. Solid State Chem. 182 (2009) 2024-2029.

[7] E. Bauer, A. Grytsiv, X-Q. Chen, N. Melnychenko-Koblyuk, G. Hilscher, H. Kaldarar, H. Michor, E. Royanian, G. Giester, M. Rotter, R. Podloucky, and P. Rogl, Phys. Rev. Let. 99 (2007) 2170011-2170014.

[8] R. Gumeniuk, W. Schnelle, H. Rosner, M. Nicklas, A. Leithe-Jasper, and Yu. Grin, Phys. Rev. Let. 100 (2008) 0170021-0170024.

[9] R. Gumeniuk, H. Rosner, W. Schnelle, M. Nicklas, A. Leithe-Jasper, and Yu. Grin, Phys. Rev. B78 (2008) 0525041-0525044.

[10] E. Bauer, X.-Q. Chen, P. Rogl, G. Hilscher, H. Michor, E. Royanian, R. Podloucky, G. Giester, O. Sologub, and A. P. Gonçalves, Phys. Rev. B78 (2008) 0645161-0645166.

[11] G. Cordier and P. Woll, J. Less-common Met. 169 (1991) 291-302.

[12] R. Marazza, R. Ferro, G. Rambaldi, and G. Zanicchi, J. Less-common Met. 53 (1977) 193-197.

[13] G. Venturini, B. Malaman, and B. Roques, J. Less-common Met. 146 (1989) 271-278.

[14] Y. M. Prots', R. Pöttgen, D. Niepmann, M. W. Wolff, and W. Jeitschko, J. Solid State Chem. 142 (1999) 400-408.

[15] Z.M.Barakatova, Y.D.Seropegin, O.I.Bodak, and S.D.Belan, Inorg. Mater. 32 (1996) 516-518.

[16] A. Imre, A. Hellmann, and A. Mewis, Z. Anorg. Allg. Chim. 632 (2006) 2217-2221.

[17] M. François, G. Venturini, E. McRae, B. Malaman, and B. Roques, J. Less-common Met. 128 (1987) 249-257.

[18] J. M. Kurenbaeva, Y.D.Seropegin, A.V.Gribanov, O.I.Bodak, and V.N.Niliforov, J. Alloys

Compd. 285 (1999) 137-142.

[19] H. Fukuoka, The Review of High Pressure Science and Technology 16 (2006) 329-335.

[20] G. M. Sheldrick, Acta Cryst. A64 (2008) 112-122.

[21] B. N. Figgis and M. A. Hitchman, Ligand Field Theory and Its Applications, Wiley-VCH, New-York, 2000, pp. 239-241.

Table 1

Crystallographic Data and Details on the Structure Determination of $SmPtGe_2$ and $Sm_2Pt_3Ge_5$

Formula	$SmPtGe_2$	$Sm_2Pt_3Ge_5$
Formula weight	490.62	1248.92
Space group	*I*mmm (No. 71)	*I*bam (No. 72)
a (Å)	4.3679(9)	10.174(1)
b (Å)	8.728(2)	11.761(2)
c (Å)	16.378(4)	6.2142(8)
V (Å^3)	624.4(2)	743.6(2)
Z	8	4
Crystal size (mm)	0.02 × 0.02 × 0.04	0.01 × 0.01 × 0.02
Diffractometer	Rigaku Raxis-Rapid	Rigaku Raxis-Rapid
Radiation (graphite monochromated)	MoKα	MoKα
X-ray absorption coefficient / mm^{-1}	81.94	91.51
2θ limit	54.9	54.9
No. of observed unique reflections	447	465
No. of variables	30	31
R_{int}	0.0504	0.0467
R, w*R*2 [a]	0.031, 0.061	0.030, 0.066
Goodness of fit, *S* [b]	1.27	1.24
Residual density (eA^{-3})	2.38/ −3.85	2.08 / −3.05

[a] $wR2 = \{\sum((Fo^2 - Fc^2)^2)/\sum w(Fo^2)^2\}^{1/2}$

[b] $S = [\sum w(|Fo| - |Fc|)^2/(No - Nv)]^{1/2}$ where *No* is the number of reflections and *Nv* is the total number of parameters refined.

Table 2

Atomic and Equivalent Isotropic Atomic Displacement Parameters of $SmPtGe_2$

Atom	*x*	*y*	*z*	U_{eq}/Å^2
Sm1	0	0	0.20309 (7)	0.0052(3)
Sm2	0	0.2414(1)	0	0.0076(3)
Pt	1/2	0.25149(7)	0.14882(4)	0.0059(2)
Ge1	0	0.3499(2)	0.1979(1)	0.0060(4)
Ge2	1/2	1/2	0.0747(2)	0.0217(7)
Ge3	1/2	0	0.0745(1)	0.0081(5)

Table 3

Anisotropic Atomic Displacement Parameters U_{ij}/Å^2 of $SmPtGe_2$

Atom	U_{11}	U_{22}	U_{33}	U_{23}	U_{13}	U_{12}
Sm1	0.0068(5)	0.0032(5)	0.0055(5)	0	0	0
Sm2	0.0066(5)	0.0088(5)	0.0074(5)	0	0	0
Pt	0.0074(3)	0.0040(3)	0.0063(3)	−0.0003(2)	0	0
Ge1	0.0038(7)	0.0049(7)	0.0093(8)	−0.0014(6)	0	0
Ge2	0.054(2)	0.0042(11)	0.0072(13)	0	0	0
Ge3	0.0163(12)	0.0035(10)	0.0045(11)	0	0	0

Table 4

Atomic and Equivalent Isotropic Atomic Displacement Parameters of $Sm_2Pt_3Ge_5$

Atom	*x*	*y*	*z*	U_{eq}/Å^2
Sm	0.27028(9)	−0.13103(7)	0	0.0082(2)
Pt1	0	0	1/4	0.0121(3)
Pt2	0.11114(7)	−0.36152(5)	0	0.0068(2)
Ge1	0	1/2	1/4	0.0067(5)
Ge2	0	0.2275(2)	3/4	0.0079(4)
Ge3	0.1549(2)	0.1052(2)	0	0.0105(4)

Table 5

Anisotropic Atomic Displacement Parameters U_{ij}/Å^2 of $Sm_2Pt_3Ge_5$

Atom	U_{11}	U_{22}	U_{33}	U_{23}	U_{13}	U_{12}
Sm	0.0117(5)	0.0077(4)	0.0053(4)	0	0	−0.0003(3)
Pt1	0.0143(5)	0.0124(5)	0.0095(5)	0	0	0
Pt2	0.0100(4)	0.0077(3)	0.0028(3)	0	0	−0.0001(2)
Ge1	0.0121(12)	0.0062(11)	0.0017(10)	0	0	0
Ge2	0.0122(9)	0.0081(8)	0.0034(8)	0	0.0016(6)	0
Ge3	0.0110(9)	0.0108(9)	0.0098(9)	0	0	−0.0002(7)

Figure captions.

Fig. 1 Crystal structure of $SmPtGe_2$ shown as a ball and stick diagram. The gray and orange filled circles represent Pt and Sm, respectively. The $Ge_{10}Pt_4$ subunit is seen in a ring. Local structures around three Ge sites are also presented.

Fig. 2 Local structure around the (a) Sm1 and (b) Sm2 sites shown in ellipsoid models (99% probability).

Fig. 3 Temperature dependence of the electrical resistivity of $SmPtGe_2$ measured by the DC four-probe method from 300 to 2 K.

Fig. 4 Temperature dependence of the magnetic susceptibility of $SmPtGe_2$. The solid line shows the theoretical values calculated using Equation (1).

Fig. 5 A ball and stick representation of the structure for $Sm_2Pt_3Ge_5$.

Figure 1

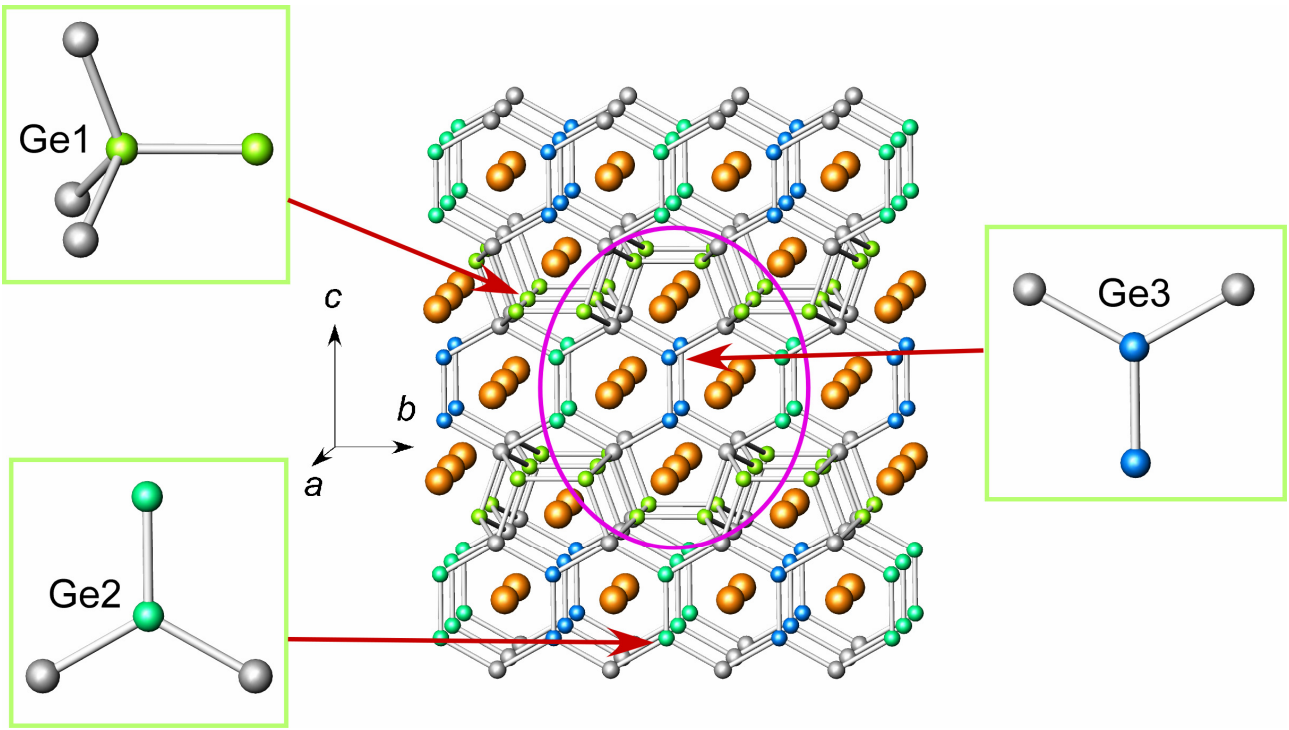

Figure 2

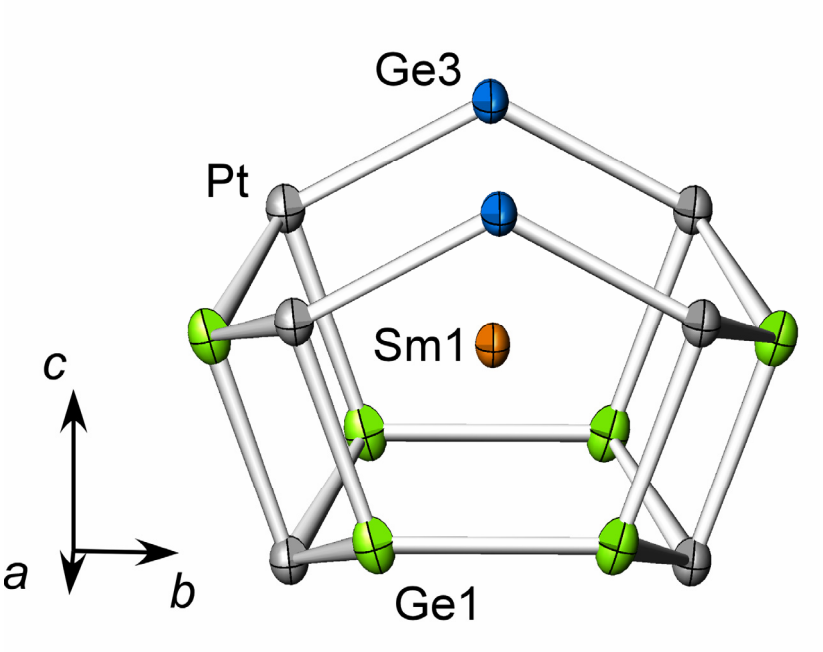

(a)

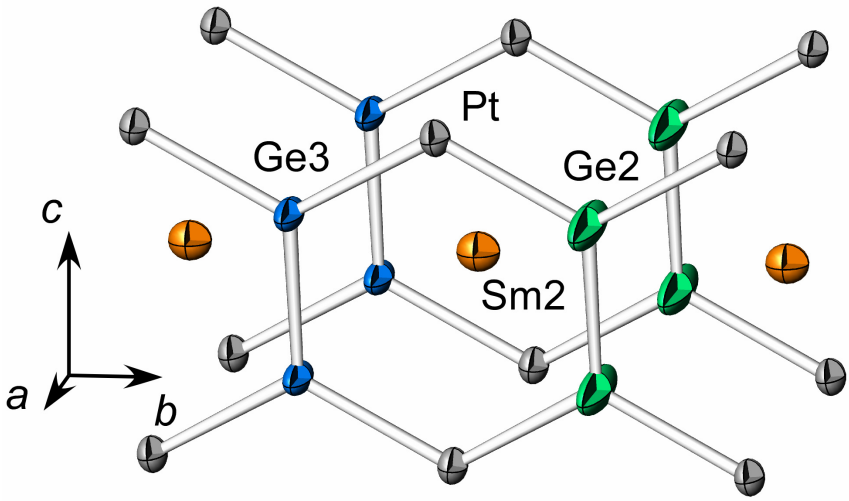

(b)

Figure 3

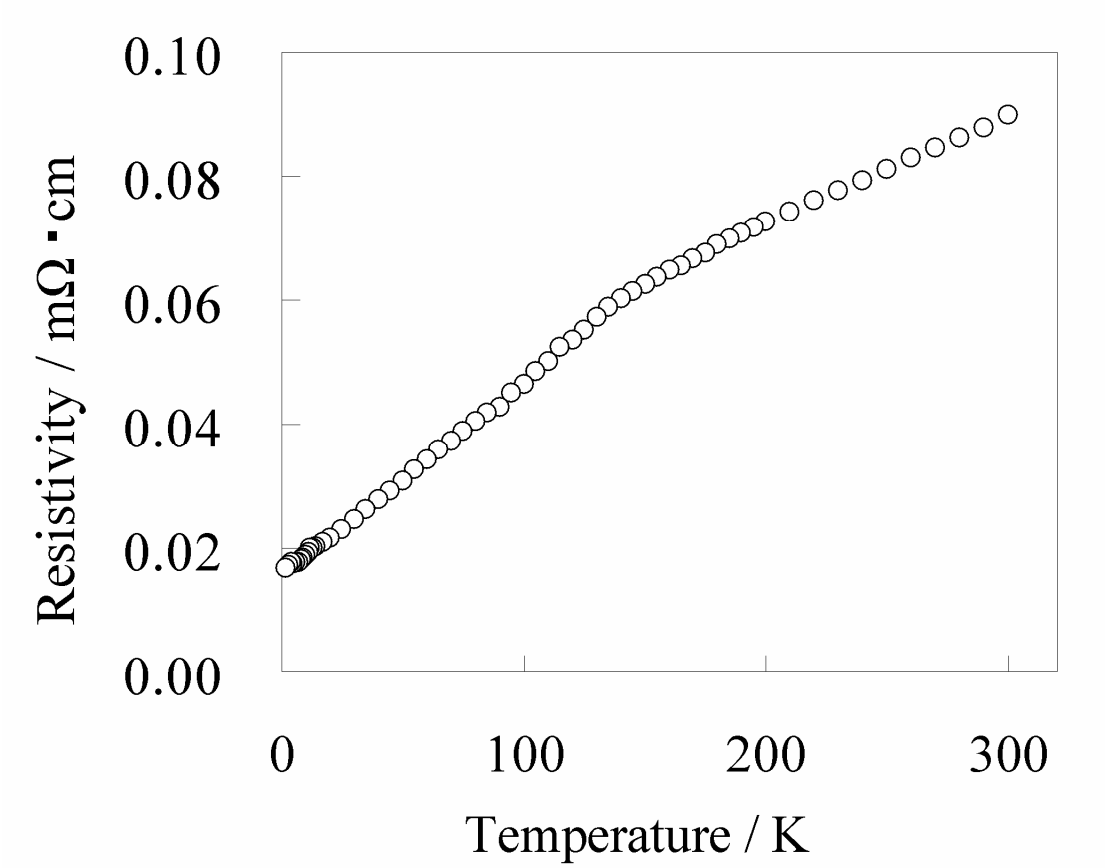

Figure 4

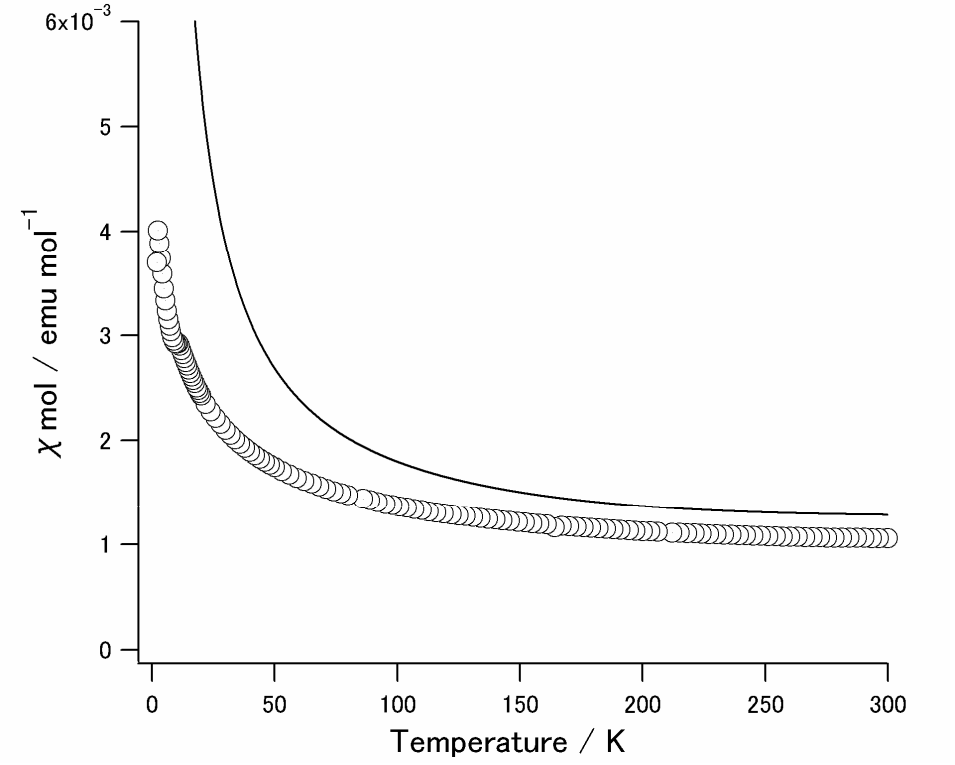

Figure 5